

Vertical-cavity surface-emitting laser (VCSEL) sources for frequency domain photon migration

Thomas D. O'Sullivan*^a, Keun-Sik No^a, Alex Matlock^a, Brian Hill^a,
Albert E. Cerussi^a, Bruce J. Tromberg^a

^aLaser Microbeam and Medical Program, Beckman Laser Institute and Medical Clinic,
University of California, 1002 Health Sciences Road, Irvine, CA 92617, USA

ABSTRACT

Frequency domain photon migration (FDPM) uses modulated laser light to measure the bulk optical properties of turbid media and is increasingly being applied for noninvasive functional medical imaging. Though semiconductor edge-emitting laser diodes (EELs) have been traditionally used for this application, we show that VCSELs exhibit performance characteristics suitable for FDPM measurements of tissue optical properties. Their output power and modulation characteristics are more than sufficient for optical property recovery. In addition, their small size, high efficiency, low cost, and simple packaging make them an attractive choice as components in clinical FDPM systems. We demonstrate a unique, compact optical probe that was enabled by VCSEL technology.

Keywords: diffuse optical imaging, VCSEL, FDPM, spectroscopy

1. INTRODUCTION

The frequency-domain photon migration (FDPM) technique is used to measure the optical absorption and scattering properties of turbid media and is under investigation for noninvasive medical imaging^{1, 2}. FDPM provides quantitative near-infrared optical absorption and scattering properties of tissue that provides functional biophysical information, such as the tissue concentrations of chromophores (e.g. hemoglobin, water, and lipid) and the size and density of cellular and subcellular components. It has been applied to a wide-range of clinical applications including studies of the human brain^{3, 4}, hemodynamic stress⁵, muscle exercise⁶, neonatal care⁷, breast tissue and tumors⁸⁻¹⁰, and others. FDPM separates absorption and scattering by precisely measuring the amplitude and phase of an intensity-modulated light wave that has propagated through turbid media, also called a photon density wave (PDW). Light sources suitable for clinical FDPM systems typically require at least 1 mW of optical power delivered to the tissue in the NIR (650-1000 nm) and modulated in the range of 50-1000 MHz. Both overall optical attenuation and source-detector separation affect the signal the noise ratio (SNR) and thus higher modulation depth (which is a function of both peak optical power and modulation bandwidth) is typically required for increased depth sensitivity and for penetrating higher attenuating tissues.

VCSELs—semiconductor lasers that emit light normal to the substrate—have not been historically applied to FDPM techniques primarily because of their perceived low output power. However, modern, commercially-available uncooled continuous-wave (CW) VCSELs output up to several hundred milliwatts depending on wavelength (650-1100+ nm) and greater than 10 W in a 2D array format. Designed for telecommunications, VCSELs are easily intensity modulated at frequencies relevant for optical property recovery and beyond. Their small size and simple packaging can enable new applications in tissue optics. In this work, we show that single VCSELs and VCSEL arrays provide sufficient optical power and bandwidth for optical property measurements in solid tissue-simulating phantom experiments and report a unique multi-color FDPM source module that was enabled by VCSEL technology.

2. METHODOLOGY

800 nm single-aperture and multiple aperture (2 x 2 array) VCSEL devices manufactured by Vixar Inc. (Plymouth, MN USA) were tested. A standard Fabry-Perot, single mode edge-emitting laser (EEL) diode was also tested for reference and comparison (LD808-SA60, Thorlabs Inc., Newton, NJ USA). All devices were mounted in 5.6mm TO packages. Benchtop testing was performed by attaching the laser to a custom PCB with backside MMCX RF connectors to

*tosulliv@uci.edu; phone 1 949 824-8838; www.bli.uci.edu

connect the high-frequency laser drive current. The devices were current controlled without temperature stabilization and were tested at room temperature. For fiber-coupled measurements, the VCSEL output was collimated with an aspheric lens and coupled to a 400 μm core silica fiber.

For modulation testing, the lasers were current modulated by using a bias tee to combine DC current injection from a standard laser driver (LDC-3916370, ILX Lightwave, Bozeman, MT USA) with an RF signal provided by a network analyzer (8753ES, HP/Agilent, Santa Clara, CA USA). DC optical power was measured using an optical power meter (PM100USB, Thorlabs Inc, Newton, NJ USA), and AC modulation was measured using a highspeed (>2 GHz) photodiode (UPD-200-SP, Alphas, Göttingen, Germany). An RF switch (HMC253QS24, Hittite, Chelmsford, MA USA) enabled dynamic selection of the laser devices.

Optical properties of tissue-simulating silicone phantoms with varying optical properties were measured using the FDPM technique. Phantom construction has been described previously¹¹. Optical properties were measured by placing a 1 x 1 mm active area avalanche photodiode (APD) module (S12060-10/C5658, Hamamatsu Corp, Shizuoka, Japan) on the surface of the phantom to collect multiply scattered photons 22 mm away from the source fiber. The network analyzer measured the frequency-dependent amplitude attenuation and phase shift of the resulting PDW relative to the source. The instrument response was calibrated by first measuring another phantom with known optical properties. Optical properties were recovered by fitting P1 approximation of the radiative transport model to the measured amplitude and phase data (50 – 500 MHz) with semi-infinite boundary conditions^{12, 13}.

A custom FDPM-module¹⁴ was modified to drive a tri-color (680, 795, and 850 nm) VCSEL package (a 5.6 mm package with 3 different wavelength VCSEL dies) manufactured by Vixar Inc. A handheld probe containing a 3 x 3 mm active area APD (S6045-05, Hamamatsu Corp, Shizuoka, Japan), custom APD module, the tri-color VCSEL package, and laser switching DC/RF circuitry was fabricated.

3. RESULTS

Table 1 displays the characteristics of the tested lasers. The peak wavelength of the lasers was measured to be approximately 800 nm. The optimal DC and RF biasing conditions were selected to maximize modulation depth at 50 MHz for optical property recovery. Figure 1 shows that the modulation bandwidth of all three lasers was comparable up to 1 GHz, which was limited by the bandwidth of the detector.

All three lasers were used to collect the amplitude decay and phase shift of tissue-simulating phantoms at a source detector separation of 22 mm and frequency range. The measured data and model fit on a single phantom are shown for all three devices in Figure 2. The lasers were used to recover the optical properties of 7 different tissue-simulating optical phantoms with varying optical properties. Table 2 displays the optical properties of the tested phantoms as recovered by the standard EEL and Figure 3 compares the results between lasers in Bland-Altman plots.

Table 1. Characteristics of the tested laser diodes and the optimal DC and RF bias to maximize modulation depth at 50MHz

| | Single Aperture VCSEL | VCSEL Array | EEL |
|-----------------------------------------------------------------------|------------------------------|--------------------|------------|
| Wavelength (nm) | 801 | 795 | 798 |
| Maximum DC optical power (mW) | 6.3 | 11.8 | >100 |
| Optimal DC current at 50 MHz (mA) | 22 | 45 | 70 |
| Optimal RF power at 50 MHz (dBm) | 13.0 | 17.7 | 10.7 |
| Optical Power at optimal bias (mW) | 6.2 | 11.6 | 17.8 |
| Total electrical power consumption (DC+RF) at optimal bias conditions | 70 | 155 | 143 |

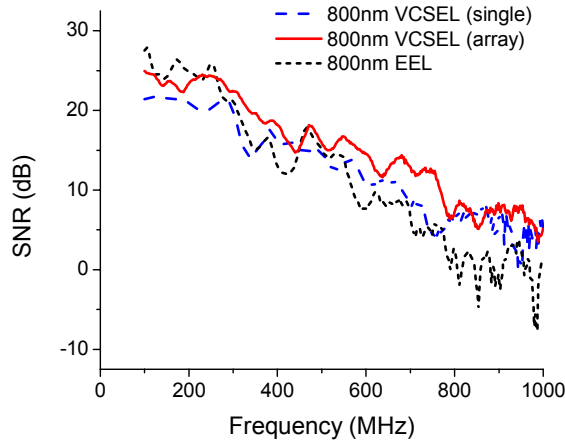


Figure 1: The modulation bandwidth of each laser measured with a high speed photodiode. The signal-to-noise ratio (SNR) was calculated by dividing the measured RF power by a prior dark noise measurement.

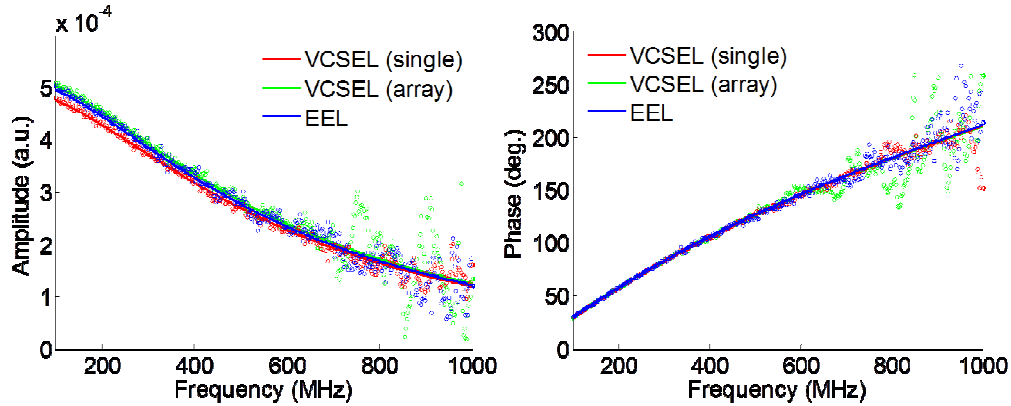


Figure 2: The calibrated amplitude and phase measured using FDPM through a tissue-simulating optical phantom ($\mu_a=0.007 \text{ mm}^{-1}$, $\mu'_s=1.01 \text{ mm}^{-1}$) at a source-detector separation of 22 mm.

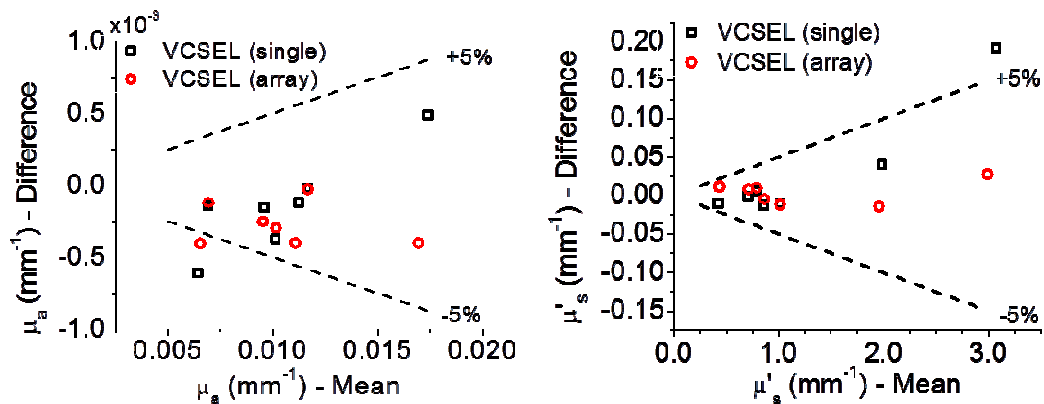


Figure 3: Bland-Altman plots which compare the optical properties recovered with the VCSEL devices (single and multiple aperture) with the standard EEL on 7 different phantoms with varying optical properties.

Table 2: Optical properties of the tested phantoms as measured using the standard EEL source

| Phantom # | μ_a (mm ⁻¹) | μ'_s (mm ⁻¹) |
|-----------|-----------------------------|------------------------------|
| 1 | 0.0070 | 1.02 |
| 2 | 0.0096 | 0.71 |
| 3 | 0.0112 | 0.87 |
| 4 | 0.0117 | 1.97 |
| 5 | 0.0103 | 2.98 |
| 6 | 0.0067 | 0.79 |
| 7 | 0.0171 | 0.43 |

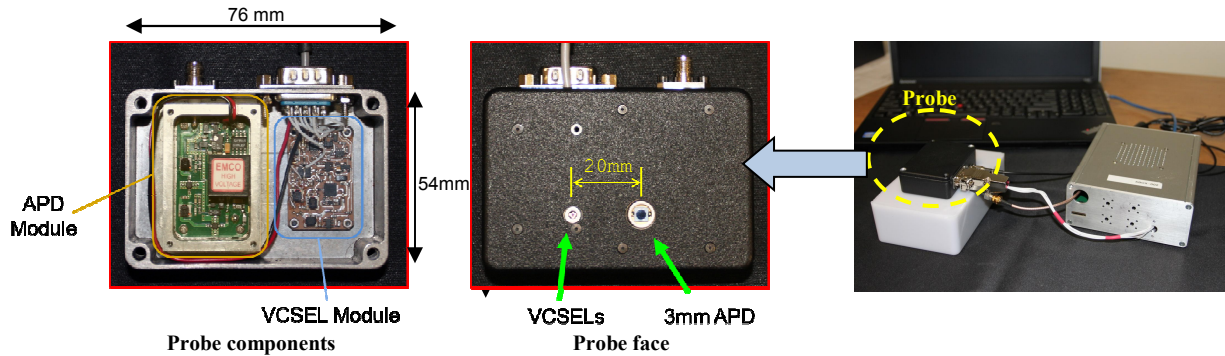


Figure 4: Prototype VCSEL-based FDPM module and integrated VCSEL/APD probe

To demonstrate how the size and geometry of VCSELS, which allows packaging of multiple sources in a single package, enables smaller and more compact FDPM probes, we developed a miniature FDPM system based on a tri-color (680, 795, and 850 nm) VCSEL package (Figure 4). The prototype system is capable of collecting FDPM measurements at a fixed 20 mm source-detector separation at frequencies 50 to 500 MHz. This system is currently undergoing validation, the results of which will be presented in a future work.

4. DISCUSSION AND CONCLUSIONS

The data demonstrate that single and multiple-aperture (array) VCSEL devices are capable light sources for FDPM recovery of optical properties in turbid media. We first examined the modulation characteristics to confirm that VCSELS can modulate as well as EEL devices. As expected, VCSELS performed similarly to the EEL over the pertinent FDPM modulation range of 50-1000 MHz. VCSEL bandwidth should be fairly equivalent or better than EELs in this range since frequency response will be limited by the parasitic limitations of the laser packaging rather than the electro-optical dynamics of the laser itself. At higher frequencies, properly designed and packaged VCSELS outperform EELs with some demonstrating data rates over 40 Gbps using direct current modulation¹⁵. We note that there was no difference in the modulation bandwidth of the single aperture VCSEL and the 2 x 2 multiple aperture VCSEL array, which suggests that VCSEL arrays are viable options for increasing optical power if required.

Next, we measured the optical properties of seven tissue-simulating phantoms with a range of attenuation using the single and multiple aperture VCSELS and the EEL. Using the EEL as a reference, VCSELS recovered the same absorption and reduced scattering coefficients within 5% in all but the highest attenuating phantom (which is difficult to measure even for the standard EEL source). Compared to the standard EEL, the single aperture VCSEL performed equivalently using 65% less optical power and 51% less electrical power.

Finally, the small size and geometry of VCSELs allow for integration of multiple dies in a single package. The miniature, dense integration of sources could be used to create FDPM imaging arrays as well as low-profile wearable FDPM sensors. To demonstrate this benefit, we fabricated a compact VCSEL-based FDPM probe. About the size of a deck of cards, the probe contains a tri-color VCSEL package, an avalanche photodiode, and the DC/RF electronics necessary to individually address the source channels—all controlled by a custom FDPM instrument module. This system is currently undergoing phantom and in vivo validation and results will be presented in a future work.

In conclusion, VCSELs exhibit performance characteristics suitable for FDPM measurements of tissue optical properties. Their output power and modulation characteristics are more than sufficient for optical property recovery. In addition, their small size, high efficiency, low cost, and simple packaging make them an attractive choice as components in clinical and next-generation wearable FDPM-based sensors.

ACKNOWLEDGEMENTS

The authors gratefully acknowledge Mary Hibbs-Brenner and Vixar, Inc. for providing the VCSEL devices for testing and characterization. This work was supported by National Institutes of Health grant P41EB015890 (Laser Microbeam and Medical Program). T. D. O'Sullivan acknowledges postdoctoral fellowship support from the NCI-T32CA009054 (University of California, Irvine Institutional Training Grant) and the Department of Defense Breast Cancer Research Program (U.S. Army Medical Research and Materiel Command W81XWH-13-1-0001). The content of this proceeding does not necessarily reflect the position or policy of the Government, and no official endorsement should be inferred. Beckman Laser Institute programmatic support from the Arnold and Mabel Beckman Foundation is gratefully acknowledged.

REFERENCES

- [1] T. D. O'Sullivan, A. E. Cerussi, D. J. Cuccia, and B. J. Tromberg, "Diffuse optical imaging using spatially and temporally modulated light," *J. Biomed. Opt.*, 17(7), 071311-14 (2012).
- [2] T. H. Pham, O. Coquoz, J. B. Fishkin, E. Anderson, and B. J. Tromberg, "Broad bandwidth frequency domain instrument for quantitative tissue optical spectroscopy," *Rev. Sci. Instrum.*, 71(6), 2500-2513 (2000).
- [3] F. Bevilacqua, D. Piguet, P. Marquet, J. D. Gross, B. J. Tromberg, and C. Depeursinge, "In vivo local determination of tissue optical properties: applications to human brain," *Appl. Optics*, 38(22), 4939-4950 (1999).
- [4] L. Meng, A. W. Gelb, B. S. Alexander, A. E. Cerussi, B. J. Tromberg, Z. Yu, and W. W. Mantulin, "Impact of phenylephrine administration on cerebral tissue oxygen saturation and blood volume is modulated by carbon dioxide in anaesthetized patients," *Brit. J. Anaesth.*, 108(5), 815-822 (2012).
- [5] T. H. Pham, R. Hornung, H. P. Ha, T. Burney, D. Serna, L. Powell, M. Brenner, and B. J. Tromberg, "Noninvasive monitoring of hemodynamic stress using quantitative near-infrared frequency-domain photon migration spectroscopy," *J. Biomed. Opt.*, 7(1), 34-44 (2002).
- [6] G. Ganesan, J. A. Cotter, W. Reuland, A. E. Cerussi, B. J. Tromberg, and P. Galassetti, "Effect of Blood Flow Restriction on Tissue Oxygenation during Knee Extension," *Med. Sci. Sports. Exerc.*, 47(1), 185-193 (2015).
- [7] A. Cerussi, R. Van Woerkom, F. Waffarn, and B. Tromberg, "Noninvasive monitoring of red blood cell transfusion in very low birthweight infants using diffuse optical spectroscopy," *J. Biomed. Opt.*, 10(5), 051401-051401-9 (2005).
- [8] B. J. Tromberg, O. Coquoz, J. B. Fishkin, T. Pham, E. R. Anderson, J. Butler, M. Cahn, J. D. Gross, V. Venugopalan, and D. Pham, "Non-invasive measurements of breast tissue optical properties using frequency-domain photon migration," *Philos. T. Roy. Soc. B*, 352(1354), 661-668 (1997).
- [9] A. E. Cerussi, V. W. Tanamai, D. Hsiang, J. Butler, R. S. Mehta, and B. J. Tromberg, "Diffuse optical spectroscopic imaging correlates with final pathological response in breast cancer neoadjuvant chemotherapy," *Philos. T. Roy. Soc. A*, 369(1955), 4512-4530 (2011).

- [10] N. Shah, A. E. Cerussi, D. Jakubowski, D. Hsiang, J. Butler, and B. J. Tromberg, "Spatial variations in optical and physiological properties of healthy breast tissue," *J. Biomed. Opt.*, 9(3), 534-540 (2004).
- [11] A. E. Cerussi, R. Warren, B. Hill, D. Roblyer, A. Leproux, A. F. Durkin, T. D. O'Sullivan, S. Keene, H. Haghany, T. Quang, W. M. Mantulin, and B. J. Tromberg, "Tissue phantoms in multicenter clinical trials for diffuse optical technologies," *Biomed. Opt. Express*, 3(5), 966-971 (2012).
- [12] J. B. Fishkin, S. Fantini, M. J. van de Ven, and E. Gratton, "Gigahertz photon density waves in a turbid medium: Theory and experiments," *Phys. Rev. E*, 53(3), 2307-2319 (1996).
- [13] R. C. Haskell, L. O. Svaasand, T. T. Tsay, T. C. Feng, M. S. McAdams, and B. J. Tromberg, "Boundary conditions for the diffusion equation in radiative transfer," *J. Opt. Soc. Am. A*, 11(10), 2727-41 (1994).
- [14] K.-S. No, R. Kwong, P. H. Chou, and A. Cerussi, "Design and testing of a miniature broadband frequency domain photon migration instrument," *J. Biomed. Opt.*, 13(5), 050509 (2008).
- [15] Y.-C. Chang, and L. A. Coldren, [Design and Performance of High-Speed VCSELs] Springer, Heidelberg, 233-262 (2013).